CHEMISTRY
A EUROPEAN JOURNAL

DOI: 10.1002/chem.200701030

Photocatalytic Cleavage of Single TiO_2/DNA Nanoconjugates

Takashi Tachikawa, Yoshiaki Asanoi, Kiyohiko Kawai, Sachiko Tojo, Akira Sugimoto, Mamoru Fujitsuka, and Tetsuro Majima*[a]

Abstract: TiO_2/DNA nanoconjugates were successfully fabricated by using the catechol moiety as a binding functional group, which was confirmed by steady-state absorption and fluorescence spectroscopies. Upon UV irradiation, the photocatalytic cleavage of the TiO_2/DNA nanoconjugates was observed at the single-molecule level by using wide-field fluorescence microscopy. The decrease in the number of conjugates, which was estimated from the luminescent spots due to semiconductor quantum dots modified at the DNA strand, was significantly inhibited by a single A/C mismatch in the DNA sequences. This result strongly suggests that the migration of holes, which are injected from the photoexcited TiO_2 into the DNA, through the DNA bases plays an important role in the photocatalytic cleavage of the conjugates. The influences of the photogenerated reactive oxygen species (ROS) on the cleavage efficiency were also examined. According to the experimental results, it was concluded that oxidation of the catechol moiety and/or the DNA damage are key reactions in this process.

Keywords: DNA · fluorescence microscopy · photocatalysis · photochemistry · single-molecule studies

Introduction

Bioconjugated nanomaterials that are composites between metal or semiconductor nanomaterials and biomolecules, such as DNA and proteins, have the potential to provide various unique and new functions in a variety of areas such as biosensors or drug and gene delivery.[1] Although the conjugations can be significant, several problems cannot be ignored, namely the undesirable reactions and byproducts, the possible toxicity or non-biocompatibility of the used materials, and the higher cost of controlled-release systems.[2] Most significantly, the adsorption and chemical-reaction dynamics presumably associated with the spatial heterogeneities of the surface and the local environments make it rather difficult for ensemble-averaged measurements to evaluate their functions.

In this study, we attempted to overcome the above-mentioned problems by investigating the photocatalytic reactions of a novel nanoconjugation consisting of TiO_2 nanoparticles and DNA at the single-molecule level. The TiO_2 photocatalysts have found a wide application in fields such as dye-sensitized solar cells, environmental purification, chemical sensors, and photodynamic therapy (PDT).[1c–e,3] Thus, much would be gained if the photocatalytic reactions at the heterogeneous interfaces could be directly monitored and controlled with both time and spatial resolutions. However, to the best of our knowledge, there is no report describing the single-molecule detection of bioconjugated TiO_2 nanoparticles.

Recently, it was reported that the catechol (CA) moiety can be used in conjunction with TiO_2 to selectively direct a light-induced charge separation to the attached DNA strands.[1c,d] Inspired by this, we selected the CA as a key feature of the synthetic DNA for the fabrication of nanoconjugates with TiO_2 nanoparticles. Here, a dopamine molecule was introduced into the 5-methylcytosine (^{Me}C) group of the DNA by postmodification (see Experimental Section for details). Also, we applied the photocatalytic oxidation of the CA moiety, which produces the non-adsorbed products, such as quinones, to release the modified DNA into solution (see reference [4] and Supporting Information for details). To detect the photocatalytically induced cleavage of single nanoconjugates upon UV irradiation, the complementary DNA strand was modified with a strongly luminescent semiconductor quantum dot (QD, Invitrogen, Qdot 605 Streptavidin Conjugate) as a probe by means of a streptavidin–

[a] Dr. T. Tachikawa, Y. Asanoi, Prof. Dr. K. Kawai, S. Tojo, Prof. Dr. A. Sugimoto, Prof. Dr. M. Fujitsuka, Prof. Dr. T. Majima
The Institute of Scientific and Industrial Research (SANKEN)
Osaka University, Mihogaoka 8-1, Ibaraki, Osaka 567-0047 (Japan)
Fax: (+81) 6-6879-8499
E-mail: majima@sanken.osaka-u.ac.jp

Supporting information for this article is available on the WWW under http://www.chemeurj.org/ or from the author.

biotin interaction (see Figure 1 and Experimental Section for details). It is expected that the moving away of the QD-modified DNA from the focus area, which is caused by the photocatalytic oxidation of the CA moiety to produce quinones, should quench the luminescence.

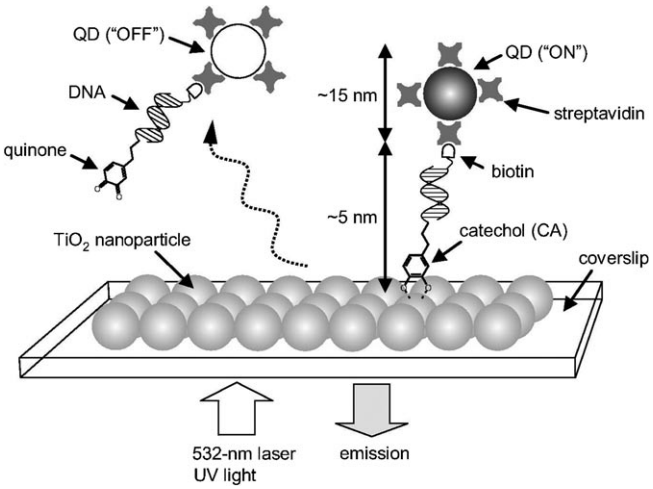

Figure 1. Optical detection of single TiO_2/DNA nanoconjugates. The moving away of the QD-modified DNA from the focus area, which is caused by the photocatalytic oxidation of the catechol (CA) moiety to produce the non-adsorbed products, such as quinones, should quench the luminescence.

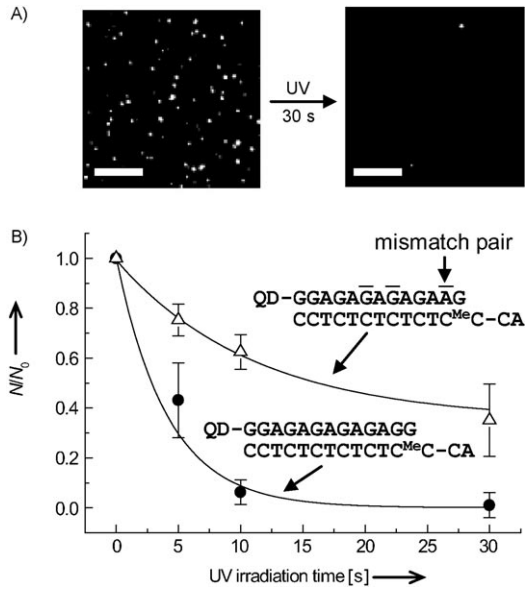

Figure 2. A) Typical single-molecule fluorescence images obtained for the fully matched DNA on the TiO_2 surface before (left) and after (right) the UV irradiation for 30 s. The bright spots are attributed to single QDs modified at the DNA. The scale bars are 10 μm. B) The UV irradiation time dependence of the N/N_0 values obtained for the fully matched and mismatched DNA duplexes. N_0 and N denote the number of luminescent spots before (over 300 spots) and after the UV irradiation, respectively. A single mismatch (A/C mismatch) is indicated by the arrow. The characteristic lifetimes of the nanoconjugates under UV irradiation were determined to be 4 and 11 s for the fully matched and mismatched DNA, respectively, by single-exponential fits. Almost a similar A/C mismatch effect on the decrease in N was observed for two different base pairs as noted by the upper lines.

Results and Discussion

Figure 2A shows the single-molecule fluorescence images observed under a 532-nm excitation before (left) and after (right) the UV irradiation (365 nm, 0.2 mW cm^{-2}) of the TiO_2 film for 30 s. Before the UV irradiation, a large number of luminescent spots were observed. Notably, no significant quenching of the QD emission in the presence of TiO_2 nanoparticles was observed due to the fact that the CdSe core is encapsulated in a shell of ZnS and a polymer. All of the control experiments, that is, in the absence of the CA moiety or TiO_2 (data not shown), the single-molecule spectral and photoblinking measurements, and the bulk measurements for the DNA-modified TiO_2 suspensions strongly support the fact that the observed spots are attributable to single QDs modified at the DNA duplex adsorbed on the TiO_2 surface through the chelating complex of the hydroxyl groups of CA with the surface Ti^{IV} ions (see below and Supporting Information).[1c,d,3d] On the other hand, only a few luminescent spots were observed after a 30-s UV irradiation (Figure 2A, right).

Several possible reasons for the decrease in the number of luminescent spots (N) upon UV irradiation should be considered as follows: 1) the photobleaching of QD, 2) the photocatalytic oxidation of the CA moiety to produce the non-adsorbed products, such as quinones,[4,5] and 3) the oxidative strand scission of DNA.[6] The reason for excluding (1) is due to the fact that a negligible bleaching was observed after the 532-nm laser irradiation (2 mW cm^{-2}) for 10 min under the same conditions.

Interestingly, as shown in Figure 2B, the decrease in N was significantly inhibited by a single A/C mismatch in the DNA sequences, strongly suggesting that the migration of holes, which are injected from the photoexcited TiO_2 into the DNA, through the DNA bases plays an important role in the decreased N. The characteristic lifetimes of the nanoconjugates during UV irradiation were tentatively determined to be 4 and 11 s for the fully matched and mismatched DNA duplexes, respectively, by single-exponential fits, although the decay profile should display a non-exponential nature that may be a consequence of the complexity and heterogeneity of the reaction dynamics. In addition, a similar A/C mismatch effect on the decrease in N was almost observed for two different base pairs as noted by the upper lines in Figure 2B.

To confirm the formation and the photocatalytic oxidation of the conjugates at the bulk level, the steady-state diffuse reflectance measurements were performed. The CA–DNA duplex (5×10^{-8} mol) was mixed with a TiO_2 suspension (4 mg ST-01 TiO_2 powder and 100 μL cacodylate buffer (20 mM, pH 7.0)), and the TiO_2 particles in the suspension

were completely separated by centrifugation using a high-speed microcentrifuge at room temperature. The resulting DNA-modified TiO_2 powder was washed twice with the cacodylate buffer, and then added to 100 μl of the cacodylate buffer.

As shown in Figure 3A, a visible absorption band appeared upon addition of the CA–DNA duplex to the TiO_2 suspension, indicating the formation of a charge-transfer complex between the CA moiety and TiO_2 (see also Supporting Information).[1c,d] We confirmed whether or not the bleaching of the charge-transfer band due to the photocatalytic oxidation in the bulk solution occurs upon UV irradiation. The light emitted from the cylindrical black-light lamp (5–10 mW) was in the wavelength range of 305–410 nm with a maximum intensity at 355 nm, which was determined by using an EPP2000 fiber-optic spectrometer (StellarNet, Inc.). Notably, free CA molecules in an aqueous solution have negligible absorption in this wavelength region. As shown in Figure 3A, it was found that the absorption due to the charge-transfer complex decreased as UV irradiation time increased. As expected, the bleaching rate observed for the fully matched DNA was high relative to that for the mismatched DNA (Figure 3B). This result is qualitatively consistent with that obtained for the single-molecule system, although the experimental methods and conditions are quite different from each other.

It should again be noted that the yield of the cleaved TiO_2/DNA nanoconjugates was changed by over 30% with only a single base mismatch (Figure 2B). This variation is much greater than that (about 10%) obtained at the bulk level for the TiO_2/DNA suspensions (Figure 3B). To clarify the adsorption behaviors of CA–DNA on the TiO_2 surface in detail, we examined the amount of adsorbed DNA by using the Cy3 dye-modified DNA (5′-(Cy3)-GGAGAGA-GAGAGG-3′; Cy3-DNA, molecular structure of Cy3 is shown in the inset of Figure 4A) as a complementary DNA strand. The single-stranded Cy3-DNA (ssCy3-DNA), double-stranded Cy3-DNA (dsCy3-DNA, i.e., in the absence of CA moiety), and double-stranded Cy3-DNA/CA-DNA (dsCy3-DNA-CA) were mixed with the TiO_2 suspensions, and the TiO_2 particles in the suspension were separated by centrifugation.

Figure 4A shows the steady-state diffuse reflectance spectra observed for the TiO_2 suspensions containing dsCy3-DNA and dsCy3-DNA-CA. The concentrations of adsorbed DNA on the TiO_2 surface after reaching adsorption equilibrium were determined on the basis of the steady-state UV-visible absorption measurements of the supernatant solutions (Figure 4B). As a result, the yields of the adsorbed DNA on the TiO_2 surface were estimated to be 5 and 13%

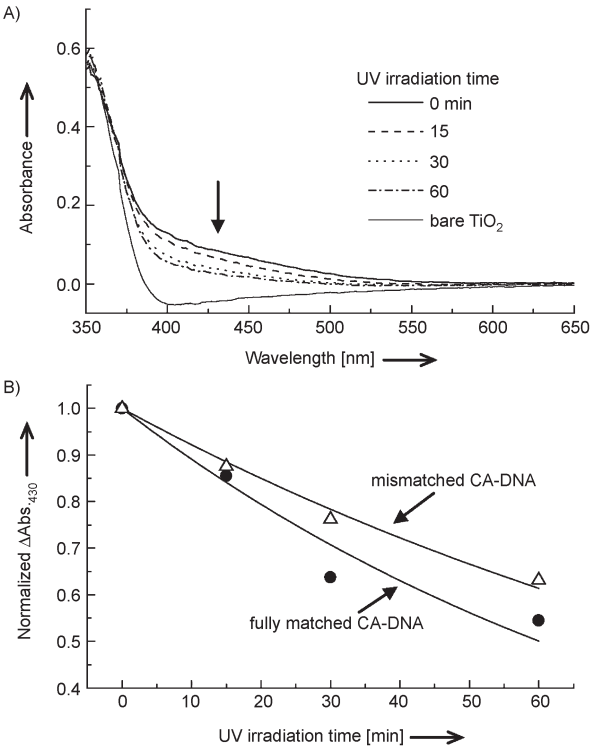

Figure 3. A) Steady-state diffuse reflectance spectra observed after UV irradiation (0, 15, 30, and 60 min) for the TiO_2 suspension (ST-01) containing the fully matched CA–DNA. The spectrum of the TiO_2 suspension in the absence of CA–DNA, i.e., bare TiO_2, is also shown. B) Normalized differential absorbance at 430 nm (ΔAbs_{430}), which is calculated by subtracting the absorbance values in the absence of CA–DNA from those in the presence of CA–DNA, observed after the UV irradiation (0, 15, 30, and 60 min) of TiO_2 suspensions containing the fully matched and mismatched CA–DNA duplexes.

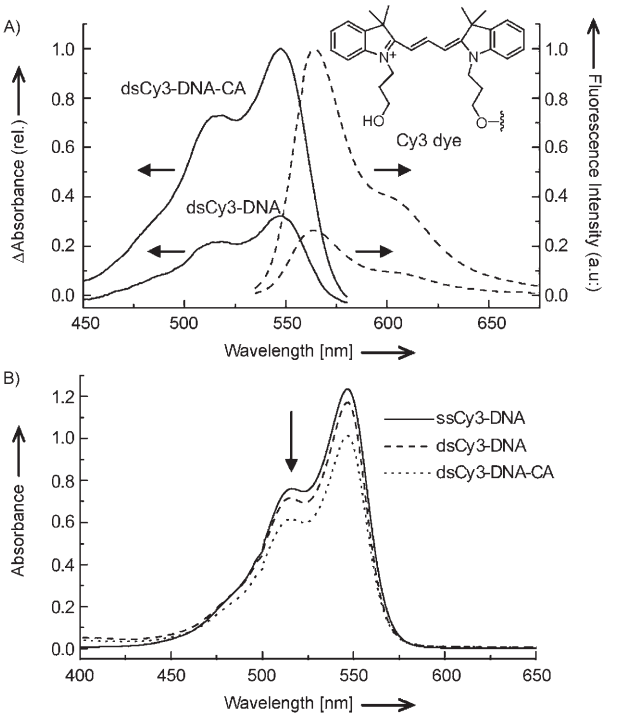

Figure 4. A) Steady-state diffuse reflectance (solid lines) and fluorescence spectra (broken lines, $\lambda_{ex}=500$ nm) observed for the TiO_2 suspensions containing dsCy3-DNA and dsCy3-DNA-CA. B) Steady-state UV-visible absorption spectra observed for the supernatant solutions of ssCy3-DNA, dsCy3-DNA, and dsCy3-DNA-CA after centrifugation.

for the dsCy3-DNA and dsCy3-DNA-CA, respectively, clearly indicating that the amount of adsorbed DNA increased in the presence of the CA moiety.

Messersmith and co-workers reported that the quinone form of CA binds much more weakly to Ti surfaces and can be removed with a lower force (ca. 200 pN) from the Ti surface relative to the enediol form (ca. 800 pN) under alkaline conditions (pH 9.7).[4b] We also found that the Langmuir adsorption constants (K_{ad}) for 3,5-di-*tert*-butylcatechol (DBCA) and 3,5-di-*tert*-butyl-1,2-benzoquinone (DBBQ) were 6500 ± 1500 and $35 \pm 20\,M^{-1}$, respectively, in acetonitrile containing TiO_2 powder (see Supporting Information for details). According to these experimental results, the observed small difference in the amount of adsorbed DNA would be partially attributable to the undesirable oxidation of the CA moiety during the experimental treatments. In addition, the excess amount of DNA molecules should result in a nonspecific adsorption on the TiO_2 surface and the possibility for changing the adsorption behaviors, that is, physisorbed and chemisorbed species. Recently, the site-specific adsorption and degradation processes of organic compounds on the TiO_2 surface were studied by solid-state NMR spectroscopy.[3d] Interestingly, the ^{13}C MAS NMR signal of the physisorbed 4-nitrocatechol was quickly reduced by UV irradiation, compared with those of the monodentately or bidentately chemisorbed species. The photocatalytic degradation mechanism of catechols at the TiO_2 surface was interpreted in terms of the interfacial charge-recombination reaction with conduction band (CB) electrons. Consequently, it is strongly suggested that in-situ monitoring of the charge-transfer dynamics within the nanoconjugates is essentially impossible at the bulk level.

When considering the TiO_2 photocatalytic reaction mechanisms,[3b,c] the influences of the photogenerated reactive oxygen species (ROS) cannot be ignored (see Supporting Information for details). As is well known that oxidative DNA damage is initiated by reaction with the ROS, such as singlet oxygen ($^1O_2$), by hydrogen-atom abstraction from the deoxyriboses to form intermediate radicals, and by the loss of electrons from the aromatic bases that form radical cations.[6]

To identify the ROS, several of the following experiments were performed: 1) in the presence of NaN_3, 2) in the presence of a hydroxyl-radical ($HO^{\bullet}$) quencher, dimethylsulfoxide (DMSO), and 3) in the presence of a superoxide ($O_2^{\bullet -}$) quencher, superoxide dismutase (SOD).[7] In all the experiments, the decrease in N upon UV irradiation was suppressed (Figure 5). In particular, in the case of NaN_3, which is an effective scavenger of $HO^{\bullet}$, $O_2^{\bullet -}$, and $^1O_2$, the decrease in N was completely inhibited.[8] On the other hand, a relatively weak inhibition was observed for the other scavengers.

TiO_2 has been used as a sunscreen agent and a photocatalyst, and has been recently suggested to be a potential photosensitizer in the fields of biomedicine, such as PDT.[9–13] Wamer et al. found that G undergoes photooxidative damage in DNA physisorbed on TiO_2 particles, resulting in the hydroxylation of G.[9] Recently, Hirakawa et al. studied the site specificity of DNA damage by anatase and rutitle TiO_2 particles by using a ^{32}P-5′-end-labeled DNA fragment obtained from the human p53 and p16 tumor-suppressor genes and the c-Ha-*ras*-1 protooncogene.[10] They found that the photoexcited TiO_2 caused mainly copper-dependent DNA damage through H_2O_2 generation in vitro. On the other hand, in the absence of Cu^{II} ions, a high concentration of anatase TiO_2 particles could induce DNA damage by the photocatalytically generated $HO^{\bullet}$. Notably, DNA can be a target molecule of the photocatalysis of TiO_2 in vivo. Serpone et al. also reported that the TiO_2 specimens extracted from commercial sunscreen lotions caused damage to both DNA plasmids in vitro and to whole human skin cells in cultures by $HO^{\bullet}$.[12] In our work, the photocatalytic oxidation of CA and/or DNA, most probably the G sites, which would cause the cleavage of the TiO_2/DNA nanoconjugate, was remarkably inhibited by the addition of scavengers such as N_3^-, DMSO, and SOD (Figure 5). Our experimental results clearly suggest that several free ROS in solution are involved in the photocatalytic oxidation processes of DNA.

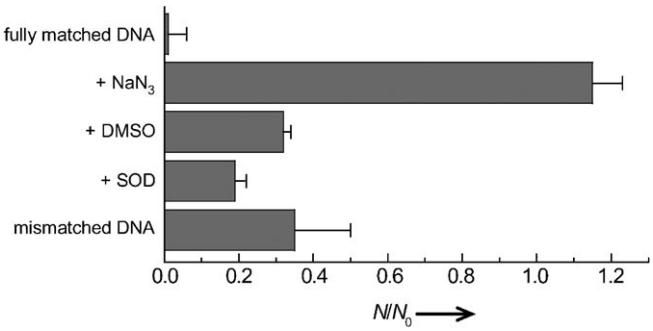

Figure 5. The N/N_0 values obtained from single-particle photoluminescence measurements for the fully matched DNA in the absence and presence of NaN_3 (100 mM), DMSO (100 mM), and SOD (5 nM), and the mismatched DNA. The UV irradiation time is 30 s.

The proposed photocatalytic reaction mechanism of the TiO_2/DNA nanoconjugate is summarized in Figure 6. Our finding implies that both the photogenerated holes in TiO_2 and the free ROS in solution are involved in the oxidation processes of the CA moiety and/or DNA itself, although it is difficult to conclude which is the most crucial reaction pathway at this time.

Recently, Lewis and co-workers determined the absolute rates of hole transfer between guanines separated by one or two A/T base pairs in stilbenedicarboxamide-linked DNA hairpins based on transient absorption measurements and theoretical calculations.[15] For instance, the forward and return hole-transfer rates from $G^{\bullet +}$ to GG separated by a single A/T base pair (GAGG sequence) were reported to be 6.0 and $1.7 \times 10^7\,s^{-1}$, respectively. Notably, the hole-transfer rate dramatically decreased due to the longer bridge consisting of two A/T base pairs separating the proximal G and the distal GG. The determined forward and return hole-transfer rates from $G^{\bullet +}$ to GG separated by two A/T base pairs (GAAGG sequence) were 4.8×10^5 and $2.4 \times 10^4\,s^{-1}$, respec-

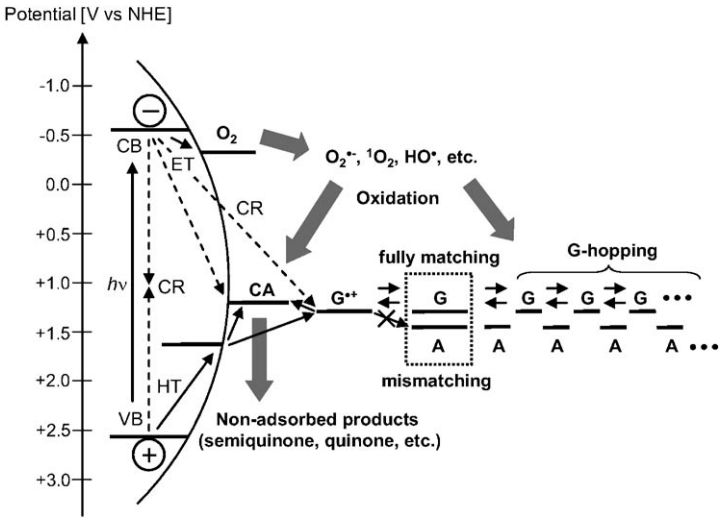

Figure 6. Proposed photocatalytic reaction mechanisms of the TiO_2/DNA nanoconjugate. The minus and plus signs denote an electron and hole, respectively. CB and VB denote the valence and the conduction bands of TiO_2, respectively. ET and HT denote the electron and hole transfer from CB and VB to the adsorbates, respectively. CR denotes the charge-recombination reaction (see dashed arrows). The oxidation potentials of the DNA bases and CA are reported in references [8b, 14a], respectively.

tively.[15] On the other hand, the charge-recombination dynamics between the surface-bound radical cations, such as $CA^{\bullet+}$, and the electrons in TiO_2 showed a wide distribution from 10^5–10^{12} s^{-1} due to the heterogeneous electron-trapping and -detrapping processes.[3d,14] These kinetic data would partially explain why we could observe a significant mismatch effect on the cleavage of the nanoconjugates upon UV irradiation, such that the formation of intermediate radical cations near the surface increases the charge recombination and thus lowers the quantum yield for degradation.[14b,16] Thus, it was considered that the spatial separation between the photogenerated charge carriers by the G-hopping of holes enhanced the oxidation efficiency of CA, which acts as a deep hole trap, because the electrons in TiO_2 are allowed to competitively react with oxygen molecules at the interface (Figure 6).[17] In other words, for the fully matched DNA duplex, the photogenerated electrons in TiO_2 would be eventually consumed by oxygen molecules before recombining with $G^{\bullet+}$, resulting in the efficient oxidation of the CA moiety. On the other hand, for the mismatched DNA duplex, the photogenerated holes should localize near the surface of TiO_2 nanoparticles, resulting in the efficient charge recombination with electrons in TiO_2. However, we need further knowledge about the charge-transfer dynamics obtained by other methods, for example, time-resolved microwave conductivity and transient absorption spectroscopy techniques, before we can discuss this in detail.

Conclusion

We have successfully observed the photocatalytic cleavage of TiO_2/DNA nanoconjugates upon UV irradiation at the single-molecule level. Notably, the present conjugates can recognize a difference in a single nucleotide. This means that the present conjugate has the potential for applications such as novel biosensing and photoinduced drug-release systems. The single-molecule (particle) optical-imaging technique will open a new window for directly observing the microscopic world in many fields ranging from fundamental physics to advanced technologies together with the development of bioconjugated nanomaterials.

Experimental Section

The catechol (CA)-modified DNA (CA–DNA) was prepared by post modification using an Applied Biosystem DNA synthesizer with standard solid-phase techniques.[18] The thymidine modified by 1,2,4-triazole was introduced at the 5′ end, and the DNA assembled by the solid-phase process was then treated with a mixture of 1 mL of dopamine·HCl in DMF (0.1 M) and 0.2 mL of triethylamine at RT for 15 min to introduce the CA group. The modified DNA was washed with DMF and acetonitrile, and then cleaved from the resin by treatment with 28% NH_3 aq at RT for 24 h. The CA is very sensitive to the presence of oxygen and easily oxidizes to the quinone form. Therefore, all procedures for the sample preparation were performed under anaerobic conditions and with shielding from the UV light as far as possible. The resulting crude product was purified by JASCO HPLC with a reverse-phase C-18 column using an acetonitrile/50 mM ammonium formate gradient. No significant absorption in the visible region due to the quinone form, i.e., 1,2-benzoquinone, was observed for the purified DNA strands modified with CA.[19] The CA–DNA strands were analyzed by MALDI-TOF mass spectrometry. CA–DNA (CA-C8T5): MS calcd for $C_{131}H_{172}N_{34}O_{83}P_{12}$: 3922.6; found: 3924.5.

The colloidal aqueous solutions of TiO_2 were prepared by the controlled hydrolysis of $TiCl_4$.[12b,20] In a typical preparation, 7.58 g of fresh $TiCl_4$ (Wako) maintained at −10 °C was slowly added dropwise over 1 h into 1 L of Milli-Q water (0 °C) in a glass beaker with vigorous stirring. The TiO_2 colloidal solution (0.3 L) was subsequently dialyzed at 4 °C (Visking-tube presoaked for 1 week in approximately 2.5 L of Milli-Q water replaced several times per day) resulting in a pH of 2.0 for the colloidal solution ($[Cl^-] < 10^{-6}$ M). Transmission electron microscopy (TEM) (JEOL, JEM-3000F) and atomic force microscopy (AFM) (Seiko Instruments, SPA400-DFM) images indicated that the mean particle size of the material was about 3–4 nm. A cleaned coverslip was spin-coated with the TiO_2 colloidal solution (10 mM, 40 μL) at 3000 rpm for 50 s, and then annealed at 200 °C for 30 min in air. Note that a high annealing temperature greater than 300 °C results in measurable luminescent artifacts that are most probably due to cracks on the TiO_2 film. The resulting TiO_2-coated coverslips were subsequently washed with Milli-Q water before the surface modification. The thickness of the TiO_2 film was estimated to be a few hundred nm, based on the TEM and AFM analyses.

The amount of adsorbed DNA using Cy3 dye-modified DNA (5′-(Cy3)-GGAGAGAGAGAGG-3′; Cy3-DNA) (JBioS, Japan) was examined. The single-stranded Cy3-DNA (ssCy3-DNA), double-stranded Cy3-DNA (dsCy3-DNA), and double-stranded Cy3-DNA/CA-DNA (dsCy3-DNA-CA) (5×10^{-9} mol) were mixed with TiO_2 suspensions, and the TiO_2 particles in the suspension were completely removed by centrifugation using a high-speed microcentrifuge (Hitachi, Himac CF16RX). The TiO_2 powder (ST-01, Ishihara Sangyo Kaisha) was a generous gift from the manufacturer. This photocatalyst has a Brunauer–Emmett–Teller surface area of 300 $m^2 g^{-1}$, a primary particle size of about 7 nm, and a crystal structure of 100% anatase. The resulting DNA-modified TiO_2 powder was washed twice with the cacodylate buffer, and then added into the buffer. The

concentrations of the adsorbed DNA on the TiO_2 surface after reaching adsorption equilibrium were determined based on steady-state UV/Vis absorption measurements of the supernatant solutions. Steady-state UV/Vis absorption and diffuse reflectance spectra were measured by using UV/Vis spectrophotometers (Shimadzu, UV-3100, and Jasco, V-570, respectively) at RT. The steady-state fluorescence spectra were measured by using a Hitachi 850 spectrofluorimeter with a xenon lamp as an excited source. The yields of the adsorbed DNA on the TiO_2 surface were estimated to be 5 and 13% for dsCy3-DNA and dsCy3-DNA-CA, respectively.

For the in-situ single-molecule fluorescence measurements, a sample flow cell, which is composed of a TiO_2-coated coverslip and a clean glass slide with a double-sided adhesive spacer, was used. A 20-mM cacodylate buffer solution (pH 7, 10 μL) of the CA-DNA/5′-biotinylated DNA duplex (JBioS, Japan) (50 nM) was first introduced into the flow cell. Note that CA–DNA is hardly adsorbed onto the TiO_2 surface in phosphate buffer in the pH range of 6–7. After incubation for 10 min at RT, the flow cell was flushed several times with cacodylate buffer, then filled with a buffer solution of streptavidin-conjugated QD (Invitrogen, Qdot 605 Streptavidin Conjugate, 15 to 20 nm in diameter) (0.1 nM) to modify the DNA with QD by a strong streptavidin–biotin interaction. The Qdot 605 Streptavidin Conjugate has a stable emission in a number of distinct buffers across a range of pH conditions. An average photoluminescence quantum yield was reported to be 0.85.[21] After incubation for 10 min at RT, the TiO_2 surface was repeatedly washed with the buffer to remove the unattached and non-specifically adsorbed DNA and QD, and then filled with the buffer. The surface density of the DNA molecules immobilized on the TiO_2 surface was determined to be about five molecules per 100 μm^2, which was not dependent on the DNA sequences. All procedures for the sample preparation were shielded from the UV light.

The experimental setup is based on using a wide-field fluorescence microscope (Olympus IX71).[22] Light emitted from a continuous-wave Nd:YAG laser (JDS Uniphase, 4611-050, 532 nm, 50 mW) passing through an objective lens (Olympus, PlanApo, 1.40 NA, 100×) was used to excite the QDs. The TiO_2 film was irradiated with a 100-W mercury lamp (Ushio, USH-102D) through a band-pass filter (Olympus, U-MWU2). The powers of the UV and 532 nm light passing through the objective lens were measured by using a power meter (Ophir, OrionTH). The fluorescence from the QDs was collected by using an oil-immersion microscope objective and intensified by an image intensifier (Hamamatsu Photonics, C8600-03) coupled to a CCD camera (Hamamatsu Photonics, C3077-70). The images were recorded at the video-frame rate of 30 frames per second, then converted into an electronic movie file by using the ADVC 1394 video-capture board (Canopus). According to the threshold criterion, the fluorescence intensities of the spots in the region of interest were analyzed by using Image J software. All the experimental data were obtained at RT.

Acknowledgement

We gratefully acknowledge Professor K. Nakatani and his colleagues (SANKEN, Osaka Univ.) for measurements of MALDI-TOF mass spectra. This work was partly supported by a Grant-in-Aid for Scientific Research (Project 17105005 and others) from the Ministry of Education, Culture, Sports, Science and Technology (MEXT) of the Japanese Government.

[1] a) E. Katz, I. Willner, *Angew. Chem.* **2004**, *116*, 6166–6235; *Angew. Chem. Int. Ed.* **2004**, *43*, 6042–6108; b) N. L. Rosi, C. A. Mirkin, *Chem. Rev.* **2005**, *105*, 1547–1562; c) T. Paunesku, T. Rajh, G. Wiederrecht, J. Maser, S. Vogt, N. Stojićević, M. Protić, B. Lai, J. Oryhon, M. Thurnauer, G. Woloschak, *Nat. Mater.* **2003**, *2*, 343–346; d) T. Rajh, Z. Saponjic, J. Liu, N. M. Dimitrijevic, N. F. Scherer, M. Vega-Arroyo, P. Zapol, L. A. Curtiss, M. C. Thurnauer, *Nano Lett.* **2004**, *4*, 1017–1023; e) N. M. Dimitrijevic, Z. V. Saponjic, B. M. Rabatic, T. Rajh, *J. Am. Chem. Soc.* **2005**, *127*, 1344–1345; f) S. J. Clarke, C. A. Hollmann, Z. Zhang, D. Suffern, S. E. Bradforth, N. Dimitrijevic, W. G. Minarik, J. L. Nadeau, *Nat. Mater.* **2006**, *5*, 409–417; g) T. Pons, I. L. Medintz, X. Wang, D. S. English, H. Mattoussi, *J. Am. Chem. Soc.* **2006**, *128*, 15324–15331; h) R. Gill, R. Freeman, J.-P. Xu, I. Willner, S. Winograd, I. Shweky, U. Banin, *J. Am. Chem. Soc.* **2006**, *128*, 15376–15377.

[2] For example, see A. Nel, T. Xia, L. Mädler, N. Li, *Science* **2006**, *311*, 622–627.

[3] a) A. Hagfeldt, M. Grätzel, *Chem. Rev.* **1995**, *95*, 49–68; b) M. R. Hoffmann, S. T. Martin, W. Choi, D. W. Bahnemannt, *Chem. Rev.* **1995**, *95*, 69–96; c) A. Fujishima, T. N. Rao, D. A. Tryk, *J. Photochem. Photobiol. C: Photochem. Rev.* **2000**, *1*, 1–21; d) T. Tachikawa, M. Fujitsuka, T. Majima, *J. Phys. Chem. C* **2007**, *111*, 5259–5275.

[4] a) E. J. Nanni, Jr., M. D. Stallings, D. T. Sawyer, *J. Am. Chem. Soc.* **1980**, *102*, 4481–4485; b) H. Lee, N. F. Scherer, P. B. Messersmith, *Proc. Natl. Acad. Sci. USA* **2006**, *103*, 12999–13003.

[5] a) It has recently been reported that the photoluminescence intensity is quenched due to the biocatalyzed formation of the *o*-quinone derivative (ref. [1h]). In the present system, however, no quenching of the QD emission by the electron-transfer reaction with the resulting quinones over a 10 nm distance was expected because no photoluminescence quenching was observed in the presence of TiO_2 (reduction potential, $E_{red}(CB) = -0.53$ V vs NHE) (ref. [5b]) and streptavidin (oxidation potential, E_{ox}(tyrosine) = +0.8–0.9 V vs NHE) (ref. [5c,d]). It seems that these results are due to the fact that the CdSe core is encapsulated in a shell of ZnS and the polymer shell. It is also noted that the $E_{red}(e^-)$ and $E_{ox}(h^+)$ values of the electrons (e^-) and holes (h^+) generated in Qdot 605 (CdSe core size is ca. 5–6 nm) upon band-gap excitation are roughly estimated to be −0.91 and +0.79 V vs NHE, respectively (ref. [5e]); b) D. Duonghong, J. Ramsden, M. Grätzel, *J. Am. Chem. Soc.* **1982**, *104*, 2977–2985; c) M. Masarik, R. Kizek, K. J. Kramer, S. Billova, M. Brazdova, J. Vacek, M. Bailey, F. Jelen, J. A. Howard, *Anal. Chem.* **2003**, *75*, 2663–2669; d) L. Havran, S. Billová, E. Palecek, *Electroanalysis* **2004**, *16*, 1139–1148; e) C. J. Wang, M. Shim, P. Guyot-Sionnest, *Science* **2001**, *291*, 2390–2392.

[6] a) W. K. Pogozelski, T. D. Tullius, *Chem. Rev.* **1998**, *98*, 1089–1107; b) B. Armitage, *Chem. Rev.* **1998**, *98*, 1171–1200; c) K. Kawai, Y. Osakada, M. Fujitsuka, T. Majima, *Chem. Biol.* **2005**, *12*, 1049–1054.

[7] The Radiation Chemistry Data Center of the Notre Dame Radiation Laboratory (web edition: www.rcdc.nd.edu/index.html). See Supporting Information for details.

[8] a) This strong inhibition effect might be due to the electron-transfer quenching of $G^{\bullet+}$ (+1.29 V vs NHE) (ref. [8b]) and/or the trapped holes at the TiO_2 surface (+1.6–1.7 V vs NHE) (ref. [1c,d]) by N_3^- because of its low oxidation potential (+1.29 V vs NHE) (ref. [8c]); b) S. Steenken, S. V. Jovanovic, *J. Am. Chem. Soc.* **1997**, *119*, 617–618; c) Z. B. Alfassi, A. Harriman, R. E. Huie, S. Mosseri, P. Neta, *J. Phys. Chem.* **1987**, *91*, 2120–2122.

[9] W. G. Wamer, J. J. Yin, R. R. Wei, *Free Radical Biol. Med.* **1997**, *23*, 851–858.

[10] K. Hirakawa, M. Mori, M. Yoshida, S. Oikawa, S. Kawanishi, *Free Radical Res.* **2004**, *38*, 439–447.

[11] a) R. Cai, K. Hashimoto, Y. Kubota, A. Fujishima, *Chem. Lett.* **1992**, 427–430; b) H. Sakai, R. Baba, K. Hashimoto, Y. Kubota, A. Fujishima, *Chem. Lett.* **1992**, 185–186; c) K. Sunada, Y. Kikuchi, K. Hashimoto, A. Fujishima, A. *Environ. Sci. Technol.* **1998**, *32*, 726–728.

[12] a) R. Dunford, A. Salinaro, L. Cai, N. Serpone, S. Horikoshi, H. Hidaka, J. Knowland, *FEBS Lett.* **1997**, *418*, 87–90; b) N. Serpone, A. Salinaro, S. Horikoshi, H. Hidaka, *J. Photochem. Photobiol. A* **2006**, *179*, 200–212.

[13] Y. Nakagawa, S. Wakuri, K. Sakamoto, N. Tanaka, *Mutat. Res.* **1997**, *394*, 125–132.

[14] a) Y. Wang, K. Hang, N. A. Anderson, T. Lian, *J. Phys. Chem. B* **2003**, *107*, 9434–9440; b) T. Tachikawa, Y. Takai, S. Tojo, M. Fujitsuka, T. Majima, *Langmuir* **2006**, *22*, 893–896; c) J. Nelson, S. A.

Haque, D. R. Klug, J. R. Durrant, *Phys. Rev. B* **2001**, *63*, 205321–205329.
[15] a) F. D. Lewis, X. Zuo, J. Liu, R. T. Hayes, M. R. Wasielewski, *J. Am. Chem. Soc.* **2002**, *124*, 4568–4569; b) F. D. Lewis, J. Q. Liu, X. B. Zuo, R. T. Hayes, M. R. Wasielewski, *J. Am. Chem. Soc.* **2003**, *125*, 4850–4861; c) K. Senthilkumar, F. C. Grozema, C. F. Guerra, F. M. Bickelhaupt, F. D. Lewis, Y. A. Berlin, M. A. Ratner, L. D. A. Siebbeles, *J. Am. Chem. Soc.* **2005**, *127*, 14894–14903.
[16] a) S. Tunesi, M. A. Anderson, *Langmuir* **1992**, *8*, 487–495; b) S. Tunesi, M. Anderson, *J. Phys. Chem.* **1991**, *95*, 3399–3405; c) C. Minero, *Catal. Today* **1999**, *54*, 205–216.
[17] Another possible explanation is that the mismatch-induced structural change inhibits the attack of the CA moiety by the free ROS in solution due to steric hindrance. However, this mechanism would be excluded because an almost similar mismatch effect on the decrease in *N* was observed for two different base pairs (Figure 3B).
[18] T. R. Webb, M. K. Metteucci, *Nucleic Acids Res.* **1986**, *14*, 7661–7674.
[19] S. Nagakura, A. Kuboyama, *J. Am. Chem. Soc.* **1954**, *76*, 1003–1005.
[20] D. Lawless, N. Serpone, D. Meisel, *J. Phys. Chem.* **1991**, *95*, 5166–5170.
[21] A. Biebricher, M. Sauer, P. Tinnefeld, *J. Phys. Chem. B* **2006**, *110*, 5174–5178.
[22] a) K. Naito, T. Tachikawa, M. Fujitsuka, T. Majima, *J. Phys. Chem. B* **2005**, *109*, 23138–23140; b) K. Naito, T. Tachikawa, S.-C. Cui, A. Sugimoto, M. Fujitsuka, T. Majima, *J. Am. Chem. Soc.* **2006**, *128*, 16430–16431; c) T. Tachikawa, H.-R. Chung, A. Masuhara, H. Kasai, H. Oikawa, H. Nakanishi, M. Fujitsuka, T. Majima, *J. Am. Chem. Soc.* **2006**, *128*, 15944–15945.

Received: July 5, 2007
Revised: October 27, 2007
Published online: November 28, 2007

